PHONONS, PHONON FOCUSSING, AND HELICON-PHONON INTERACTION

K. S. VISWANATHAN
Department of Physics, Kerala University, Kariavattom, Trivandrum 695 581, India

1. INTRODUCTION

THE term phonon signifies a quantized acoustic oscillation and is of twentieth century origin. But the basic foundations of the propagation of elastic waves in isotropic media of crystals were laid more than a century ago. The subject of phonons has retained its vitality, despite sustained activity over hundred years, essentially because phonons constitute a very fundamental excitation in physics. Developments in computers, lasers, cryogenics, measuring techniques and the availability of new exotic materials have all helped the experimenter to explore frontier regions, which he could not have dreamt of attempting a few decades back, and have contributed to the phenomenal growth of the subject during last few years.

2. ELASTIC WAVES IN CRYSTALS

In an elastically isotropic medium, the waves that propagate are the shear or the compressional modes. The two shear modes propagating in any direction are degenerate but are strictly transverse in the sense that their polarization is perpendicular to the direction of propagation. Likewise the compressional mode is longitudinal or a so called 'pure mode'. In a crystal too, three types of elastic waves propagate in any direction, which we shall call for convenience the quasi-longitudinal (L), fast shear (FT) and the slow shear (ST) modes. The velocities of these waves depend on the direction of propagation as well as the elastic constants of the medium. But unlike an isotropic solid, wave propagation in crystals is anisotropic and this anisotropy bestows them with several properties, which are still being investigated. Elastic waves in crystals are not strictly longitudinal or transverse in contrast with an isotropic substance. The polarizations of the three modes mentioned above are mutually perpendicular to each other but excepting for certain special directions depending on the symmetry of the crystal lattice, these are obliquely inclined to the direction of propagation. Pure modes[1] occur along directions related to the symmetry axes, and symmetry planes, or along certain non-symmetry directions determined by the elastic constants of the crystal. Generally waves propagating along three-fold, four-fold or six-fold axes are pure and besides, there exists one pure shear mode normal to a plane of symmetry.

An important consequence of the elastic anisotropy of crystals is that the group velocity is not collinear with the wave vector except along a few symmetry directions. The group velocity vector is alternatively called the ray vector or the energy flux vector since it signifies the direction of transport of elastic energy in the medium. If a pulse of acoustic energy is radiated by a plane wave transducer, the wave packet will travel along the direction of the group velocity vector (V_s), which will be inclined to the wave vector. In order to intercept the acoustic pulse[2], the receiv-

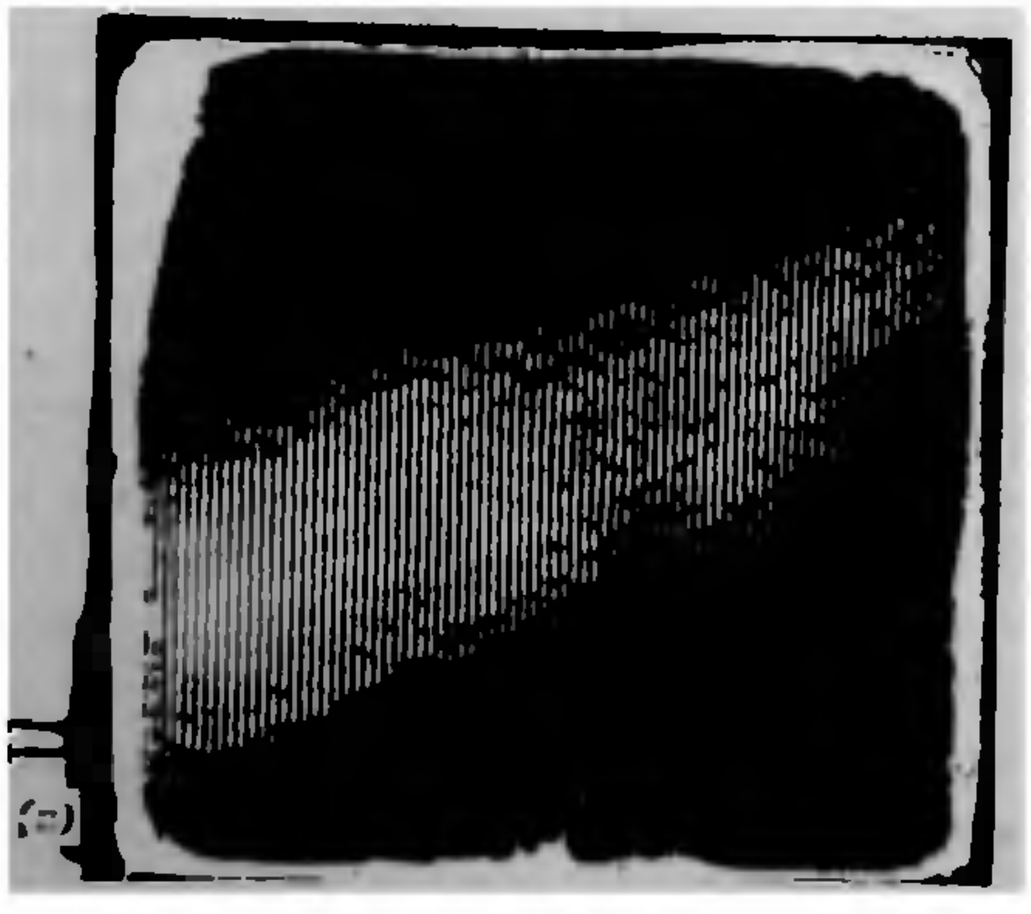

Figure 1. Deflection of the quasilongitudinal beam quartz (After staudt and look)

ing transducer should be displaced as shown in figure 1.

The anisotropy of elastic wave propagation is best understood with the aid of a few surfaces in three dimensions. If one joins the end points of all the radius vectors given by $\mathbf{r} = \mathbf{n}/v$, where $\mathbf{n}$ is a unit vector in the direction of wave propagation and v is the velocity of propagation in that direction, the surface obtained is known as the inverse velocity surface. Corresponding to the three different modes of propagation, the inverse surface exhibits three sheets. The shape of these sheets instantly shows the anisotropy in the velocity of propagation of elastic waves in any direction. Another surface, known as the energy surface or the group velocity surface, represents the envelope of all points reached by the energy flux of a disturbance set at the origin, after unit time. The radius vector from the source to any point on this surface represents the distance travelled by the energy in unit time in that direction or the group velocity of the waves. This surface exhibits topologically interesting geometric features for most crystals. The energy surfaces for the two shear modes exhibit ramps or ridges. A section of the energy surface for the ST mode by a principal plane invariably exhibits cusps along one of the symmetry axes. A cusp reveals the fact that the group velocity is a many valued function of the wave vector and there exist several wave vectors corresponding to a single group velocity vector. In figures 2 and 3, we reproduce some typical sections of the inverse velocity as well as the energy surface by the principal (100) and (110) planes[3]. The cuspidal edges seen in the figure arise only for the two quasi-shear modes; the quasi-longitudinal wave sheet does not contain a cusp. The cusps arise from the convoluted form of the quasi-shear inverse velocity surface in the vicinity of the cubic axes of the crystal. For

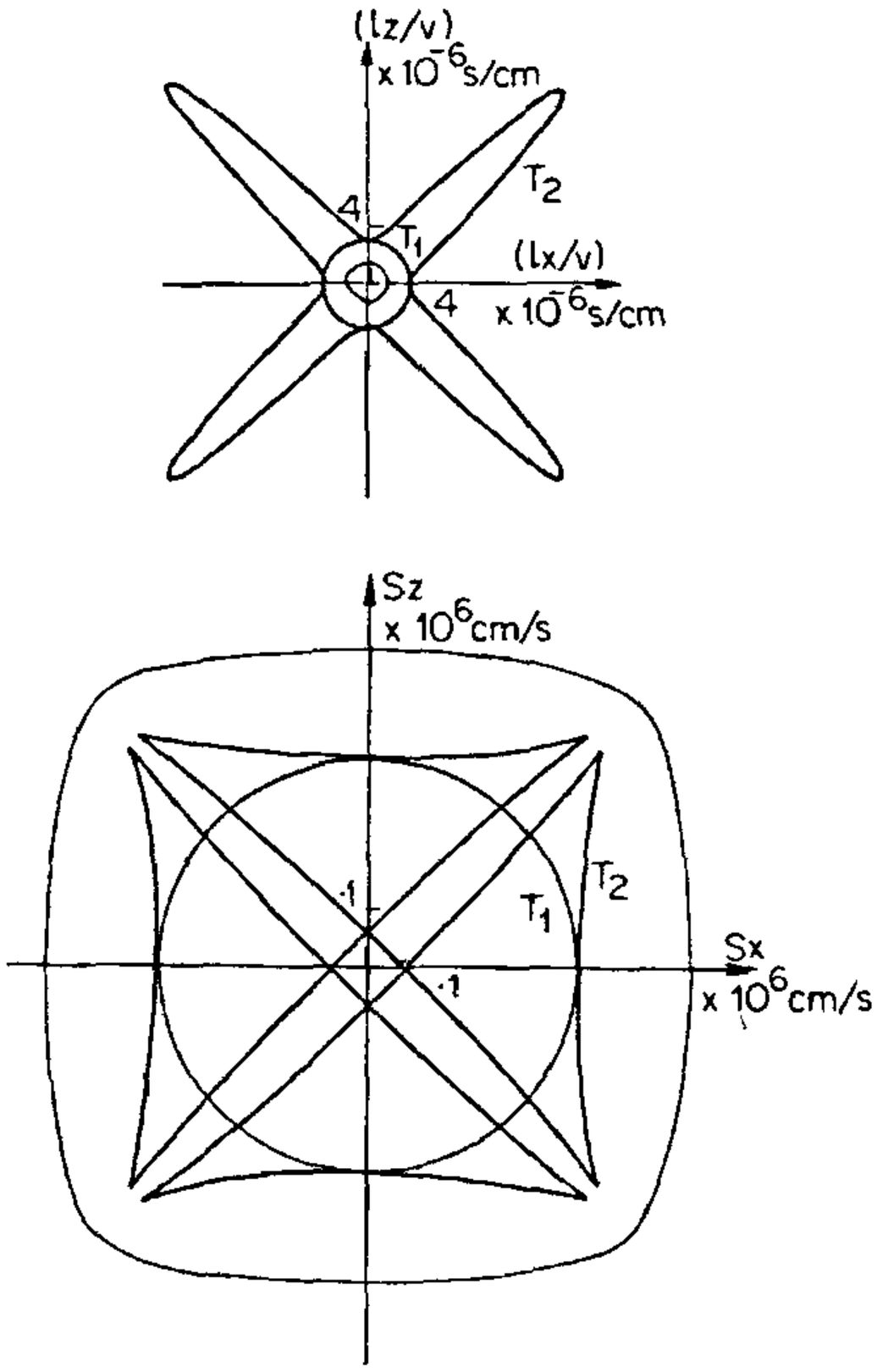

Figure 2. (a) Inverse velocity surface of V_3Si at 4.2° K in the (001) plane. (b) Ray velocity surface of V_3Si at 4.2° K in the (001) plane.

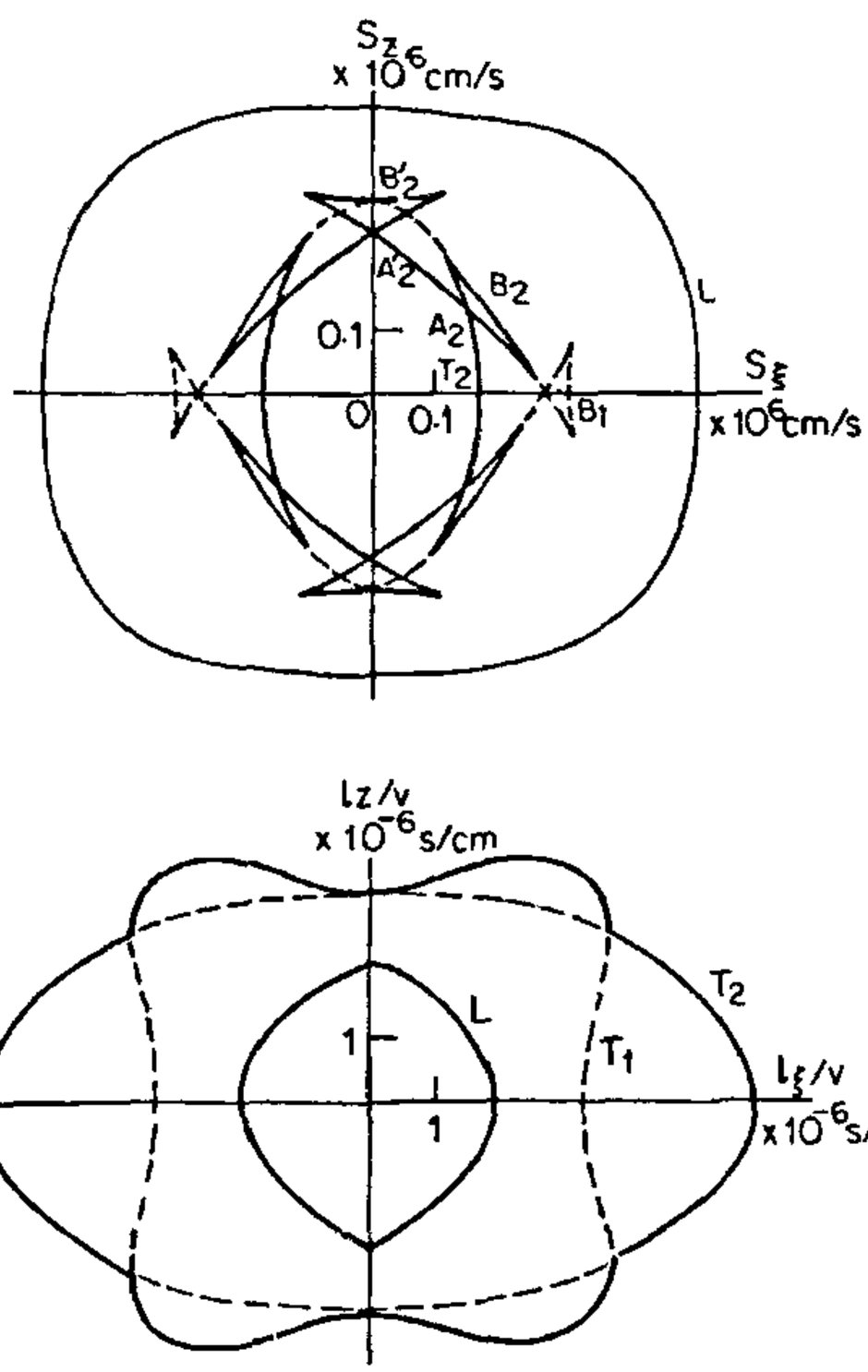

Figure 3. (a) Ray velocity surface and inverse velocity surface for Cu in the (110) plane.

sections by the principal plane for a cubic crystal, the existence of a cusp along the cubic axes or the face diagonal direction depends on the anisotropy factor $A = 2C_{44}/(C_{11} - C_{12})$. If $A > 1$, a cusp occurs along the cubic axis; otherwise, it occurs along the face diagonal.

The elastic wave surfaces are especially interesting for the A-15 compounds which have high superconducting critical temperatures. These surfaces undergo a phase transformation at low temperatures just above the superconducting critical temperatures and the shear modes propagating along a face diagonal (1 1 0) with (1 T 0) polarization becomes soft. In figure 4, we have drawn the inverse as well as the ray velocity surface[4] for V_3Si, which is one of the A-15 compounds.

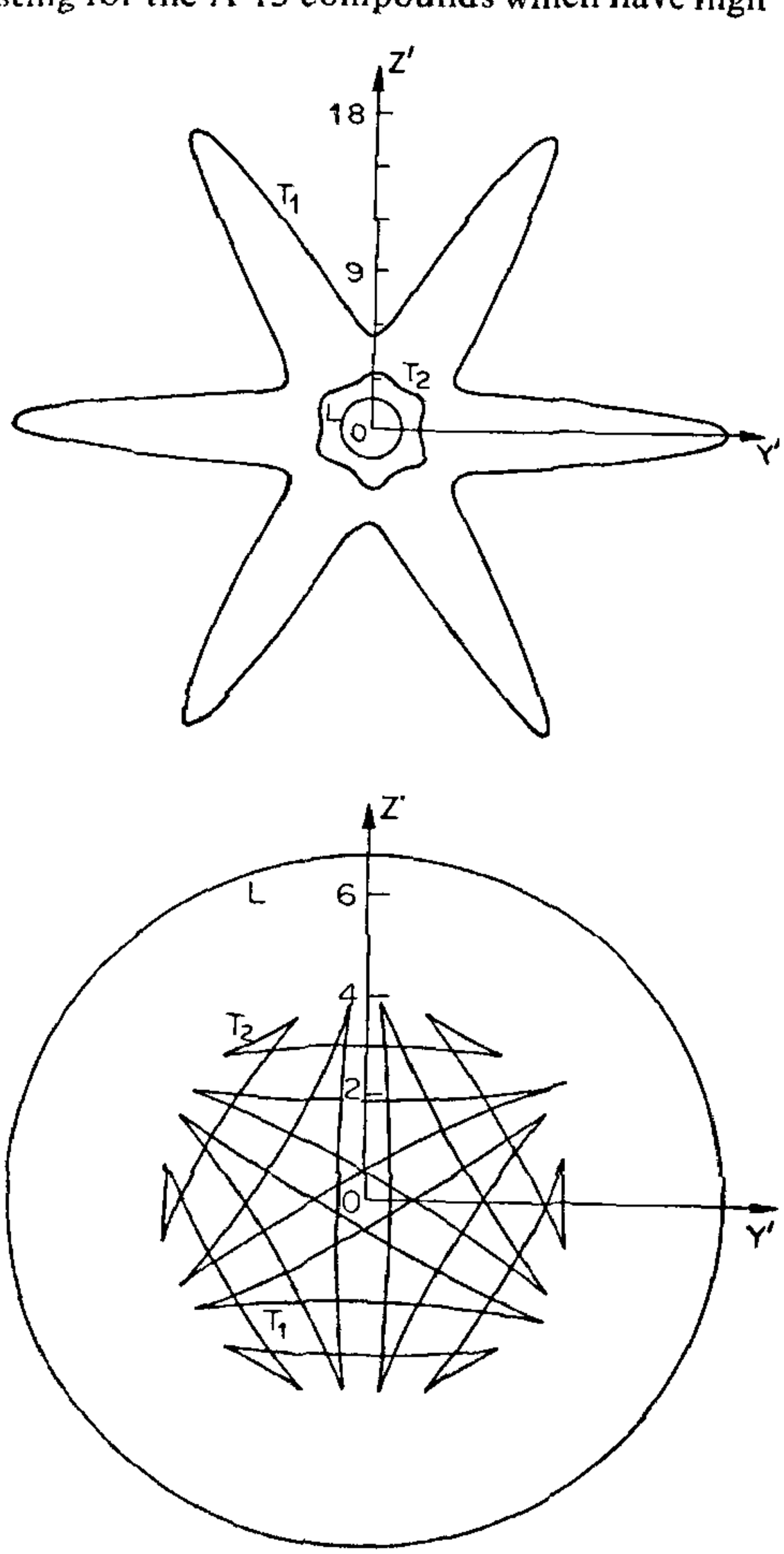

Figure 4. (a) Section of the inverse velocity surface of V_3Si at 4.2° K by the (1 1 1) plane. Y' and Z' refer to the $(\bar{1}\,1\,0)$ and $(\bar{1}\,1\,2)$ directions. (b) Section of the energy surface of V_3Si at 4.2°. Y and Z' refer to the (1 1 0) and $(\bar{1}\,1\,2)$ directions of the crystal.

3. INTERNAL CONICAL REFRACTION OF ACOUSTIC WAVES.

With the progress in experimental techniques in ultrasonics, it has become possible to observe several phenomena that have been known only in optics for a long time. As an example of the one such phenomenon, we may cite the internal conical refraction of acoustic waves. For cubic crystals, the phase velocities of the two quasi-shear modes become equal for propagation along the (1 0 0) or (1 1 1) directions. Such a direction for which the shear mode velocity is degenerate is called an acoustic axis. For propagation along an acoustic axis of a crystal of any symmetry, the polarization vectors of the shear modes can lie anywhere in a plane normal to the polarization of the longitudinal wave. The associated ray vectors emerge along the generators of a cone. Musgrave[5] showed that a circular cone of internal refraction exists for transverse waves travelling along the (1 1 1) direction of cubic crystals. The nature of conical refraction and the semiangle of the cone have been investigated for tetragonal and hexagonal crystals by the present author[6]. De Klerk and Musgrave[7] observed experimentally conical refraction for cubic crystals along the (1 1 1) direction. Papadakis[8] showed evidence of ICR in rocksalt and calcite single crystals by observing along one of the axes of threefold symmetry in each crystal. For cubic crystals, calculations show that the semi angle of conical refraction varies from 6° for aluminium to 31° for copper.

4. FARADAY ROTATION OF ACOUSTIC SHEAR MODES.

Faraday rotation and rotary activity cause the plane of polarization of linearly polarized trans-

verse waves to rotate as the wave propagates in the medium. It is well known that if the velocities of propagation of the two waves with positive and negative circular polarization are different, rotation effects occur for the plane of polarization. Though optical activity has been known since 1811, experimental evidence for acoustic activity was not forthcoming until 1970. Pines[9] as well as Joffrin and Levelut[10] provided observational evidence of rotary activity for shear waves propagating along the z axis for trigonal quartz. Theoretically rotary activity for acoustic waves is possible if the compliance matrix for a substance becomes non-symmetric and this happens for trigonal quartz, which is acoustically active for propagation along the z axis. In the absence of spatial dispersion, shear waves propagating along the z axis of a trigonal crystal are degenerate but spatial dispersion couples these modes, leading to nondegenerate circularly polarized waves propagating along the z axis.

5. HELICONS AND HELICON-PHONON INTERACTION.

It has been predicted by the present author[11] that acoustical activity can also be observed under another circumstance when the phonons interact resonantly with an electromagnetic excitation known as the helicon. While electromagnetic waves cannot normally propagate freely without suffering reflection at the surface or damping in a metal, the situation becomes different when a magnetic field is superposed on the metal. Helicons are the simplest kind of waves propagating in a magnetised plasma. The possibility of guided propagation of electromagnetic waves along a field line in a metal was first pointed out by Aigrain[12] and these waves were later observed by several others. Helicons are low frequency circularly-polarized electromagnetic waves that propagate freely in metals or doped semi-conductors. They can propagate either parallel to the magnetic field or at a small angle relative to the field. The dispersion equation for the helicon is of the form (ii)

$$\omega = \frac{k^2 CH|\cos\phi|}{4\pi Ne}\left|1-\frac{i}{\omega_c \tau \cos\phi}\right| \qquad (1)$$

where ω and k denotes the frequency and wave vector of the wave; H is the applied magnetic field; N is the density of the free electrons; ω_c is the cyclotron frequency; τ is the collision time and ϕ is the angle between the wavevector and the field. The phase velocity of the helicon is

$$u = [\omega CH|\cos\phi|/4\pi Ne]^{1/2} \qquad (2)$$

It can be seen that the helicon velocity exhibits a parabolic increase with H, the magnetic field.

6. HELICON-PHONON INTERACTION.

For magnetic fields of the order of 10^5G, the phase velocity of the helicon can be made to match the velocities of propagation of the acoustic waves in metals and interesting resonant interaction effects then take place. As stated earlier, the spectrum of helicon is quadratic with respect to the magnetic field whereas the spectrum of sound waves is linear. The dispersion curves can cross and the crossing point corresponds to a resonance. The interaction of both the waves with the conduction electrons removes the degeneracy and the result is a set of coupled electromagnetic and acoustic waves. The helicon-phonon interaction was first experimen-

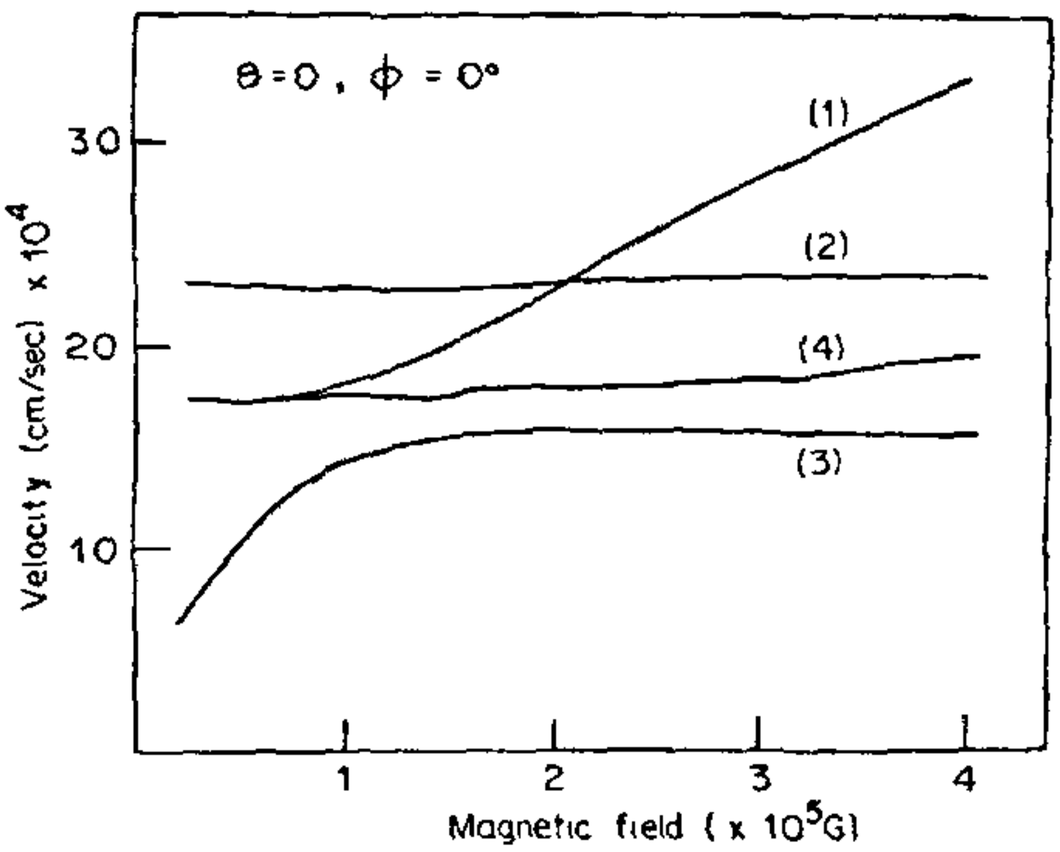

Figure 5. Variation in the phase velocity of the helicon and acoustic modes with magnetic field for Potassium; θ is the angle between the wave vector and the x axis (cubic axis), while ϕ is the angle between the magnetic field and the direction of propagation.

tally observed by Grimes and Buchsbaum[14] for Potassium.

The dispersion equation for helicon-phonon interaction for propagation of the waves parallel to the magnetic field as well as at small angles to it has been derived by the author and his students[15,16], and the nature of the interaction in the resonant region has been extensively investigated in a series of papers[17-20]. It is found that in the resonant region, strong interaction takes place between helicons and the phonons resulting in modes that are hybrid in nature and exhibit characteristics of both electromagnetic as well as elastic vibrations. Besides, at the resonant point mode conversion takes place but if one moves away from the resonance region, the waves resume their normal characteristics. In figures 5 and 6, we depict the nature of variation

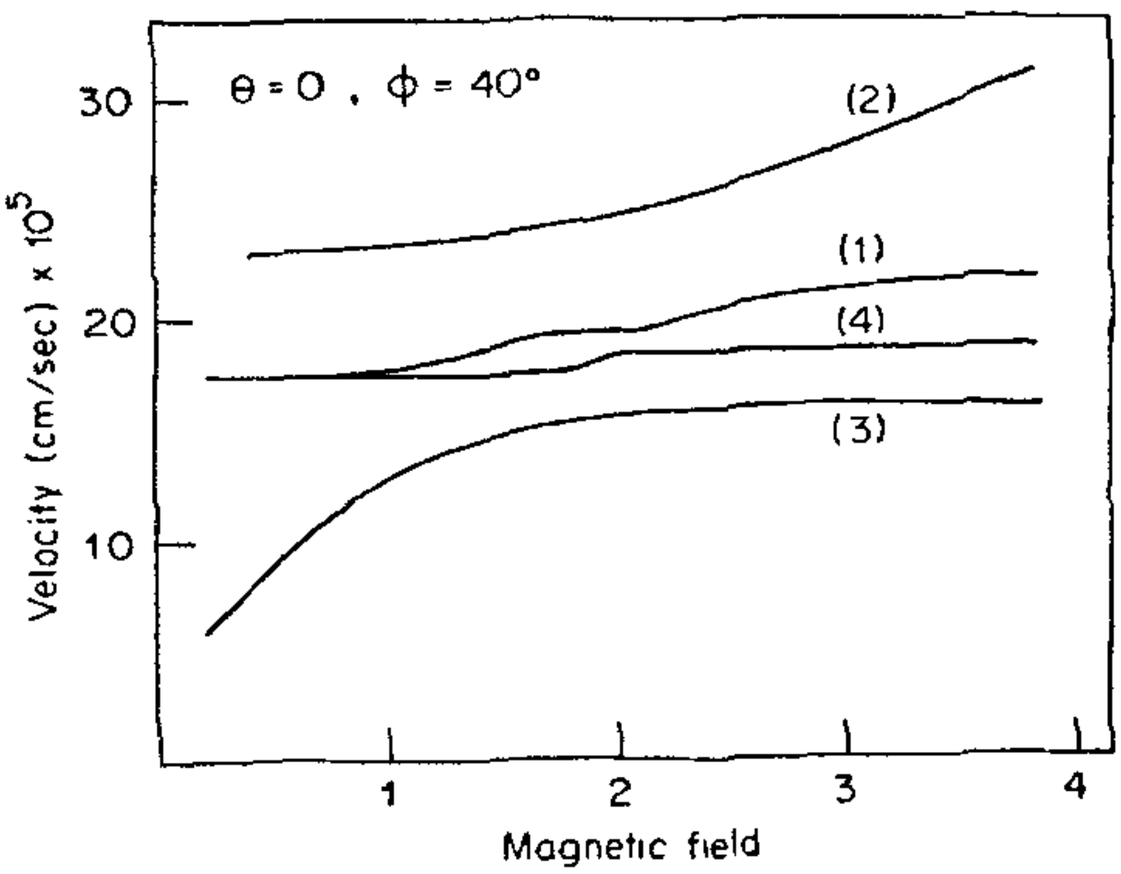

Figure 6. Variation in the phase velocity and acoustic modes with magnetic field for Potassium; $\theta = 0$, $\phi = 40$.

of the three acoustic modes, and the helicon with the magnetic field in the resonant region for parallel propagation as well as propagation of the wave at an angle 40° to the direction of the magnetic field. It can be seen that at the resonance region, mode conversion takes place and the waves exist as hybrid waves exhibiting the characteristics of both elastic as well as electromagnetic excitations. Another interesting feature is that for parallel propagation, the helicon does not interact with the longitudinal sound wave. For oblique propagation, the longitudinal displacement is no longer parallel to the magnetic field and can produce an induction field which results in interaction with the helicon. This can be seen from figure 6. As the field strength is increased, the helicon interacts successively with the slow shear, fast shear and the longitudinal mode. A significant feature of the oblique propagation is that the modes stay as hybrid waves over a longer range of the magnetic field.

When the helicon propagates at an angle to the magnetic field, there can be sigificant non-local effects and the helicon mode will be damped due to a collisionless absorption of the wave by the conduction electrons. In the long wavelength limit $kl \gg 1$, where l is the mean free path of the electrons, the dispersion equation for the helicon is modified into

$$\omega = \frac{K^2 CH}{4\pi Ne} |\cos\phi| (1 - i\Gamma) \tag{3}$$

$$\text{where } \Gamma = \frac{1}{\omega_c \tau \cos\phi} + \frac{3}{16} . kR \sin^2\phi \tag{4}$$

Non-local effects do not alter the helicon spectrum but modify the damping. The first term in (4) is the collisional damping whereas the second term denotes non-local damping which is collisionless. When further quantum effects become significant, the damping displays yet another interesting feature. In a strong magnetic field, the electron energy levels are quantized and the separation between these Landau levels is $\hbar\omega_c$ which is usually less than the Fermi energy E_F. The transport properties of a metal are determined by electrons in a narrow region of width T near the Fermi surface. Under conditions of quantization, the values of the component parallel to the field (z) can take only discrete values given by

$$P_z = 2m^* (E_F - n\hbar\omega_c)^{1/2} \tag{5}$$

It then becomes possible that for some values of the magnetic field, there may be no electrons in the Fermi surface with a P_z value satisfying conservation conditions. In these regions of the

magnetic field, there will be no absorption of the wave and the damping will be zero. Damping will be finite only for certain discrete values of the magnetic field for which the electrons on the Fermi surface with P_z given by (5) satisfy the conservation conditions. Thus the damping will undergo oscillations with the magnetic field and these are known as the giant quantum oscillations. Returning to helicon-phonon interaction, all the four hybrid modes including the three acoustic modes exhibit damping due to collisionless absorption. This is shown in figure 7

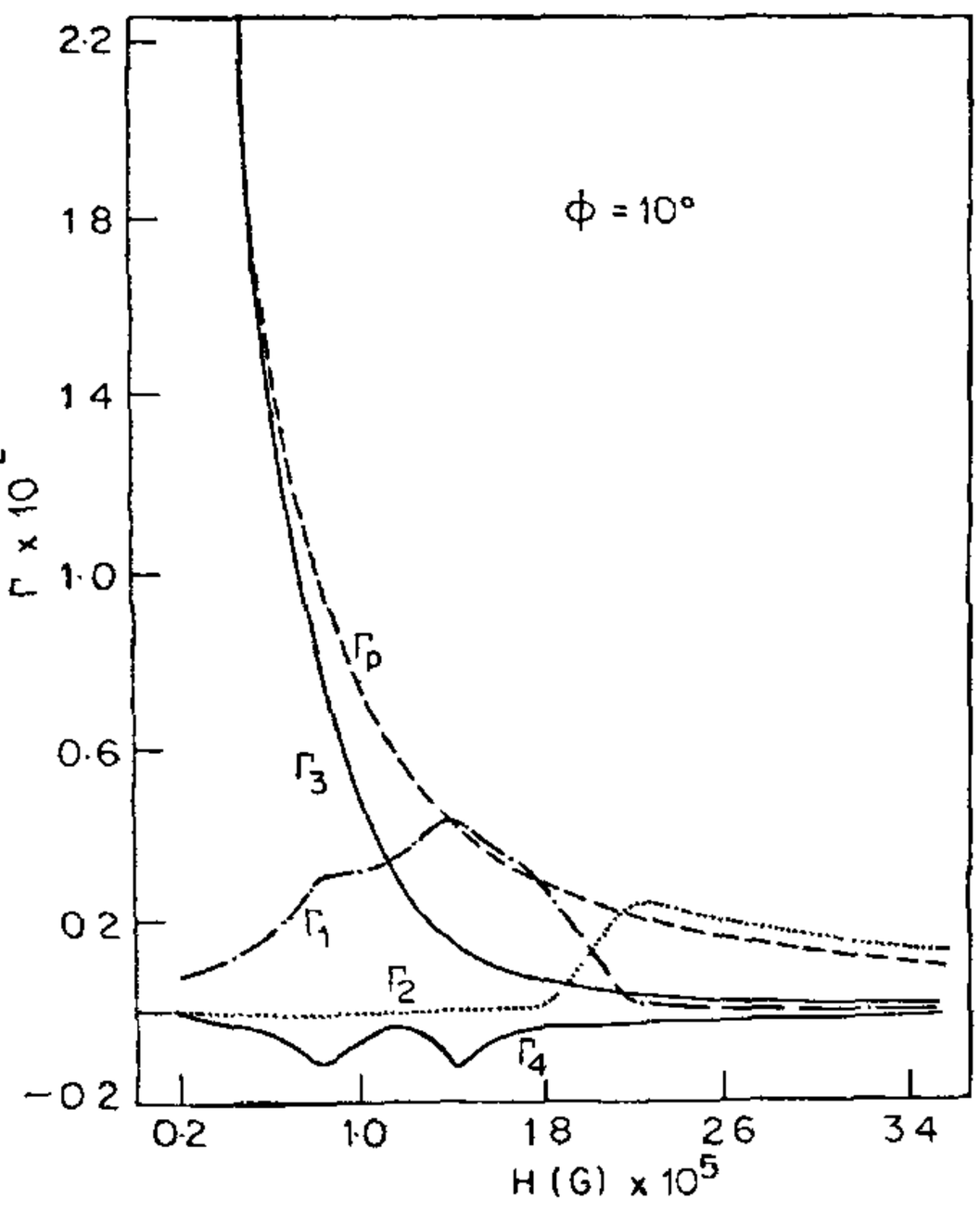

Figure 7. Variation in the damping decrement with magnetic field.

where Γ_p denotes the damping of the helicon in the absence of interaction; Γ_1, Γ_2,Γ_3,Γ_4, denote the damping factor of the four hybrid modes. The figure clearly shows that the acoustic modes also get damped in the interaction region, besides confirming the phenomenon of mode conversion mentioned earlier. Further all the four modes exhibit giant quantum oscillations in the interaction region, which is normally a property of the helicon alone. This is shown by figure 8 where the modes (Γ_1 Γ_3) exhibit giant quantum oscillations.

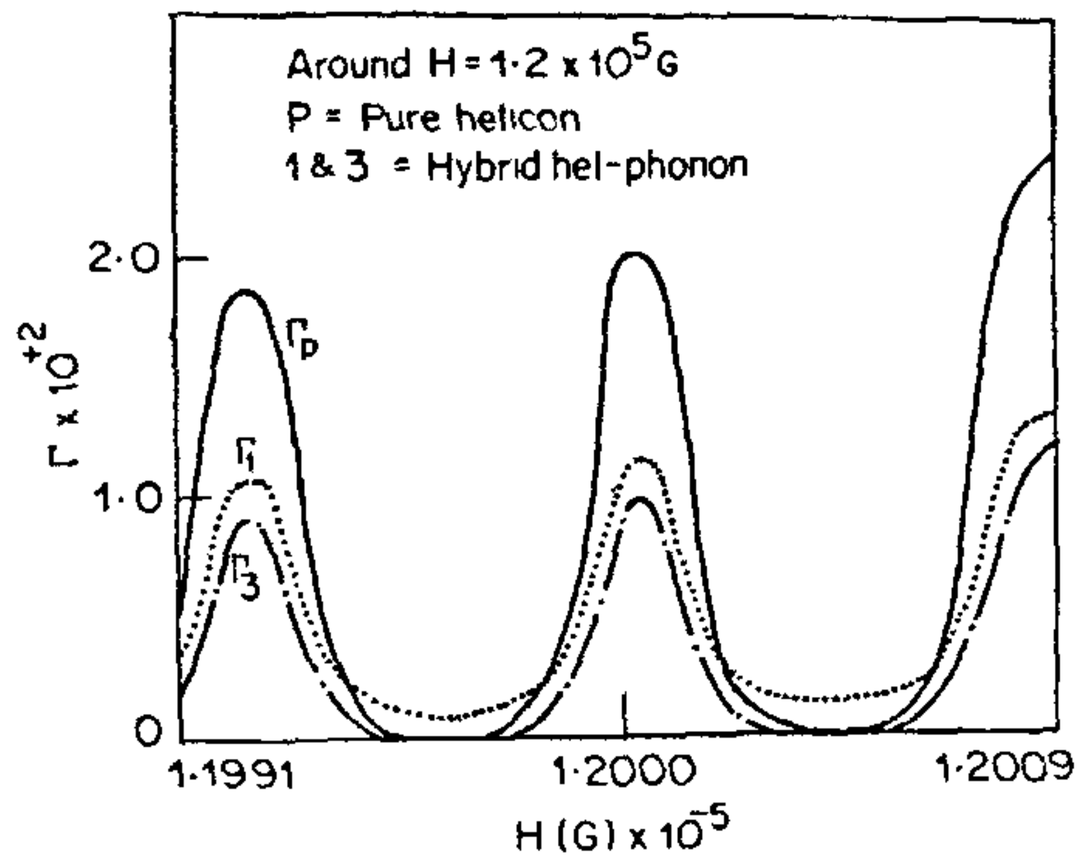

Figure 8. Giant quantum oscillations in the damping of the hybrid modes with magnetic field.

As a result of the helicon-phonon interaction, the degeneracy in the velocity of the two shear modes propagating along a cubic axis in a metal is lifted. Consequently the two shear modes, which are circularly polarized will propagate with different velocities, the difference in the velocities depending on the strength of the helicon-phonon interaction. Hence the conditions for rotary activity are present and the rotary activity of the shear modes can be observed, if looked for under proper experimental conditions.

7. PHONON FOCUSSING IN CRYSTALS

When a metal is cooled far below the superconducting critical temperature, there are negligible normal state electrons to carry heat so that thermal transport is dominated by phonon scattering processes. If the substance is further free from defects, impurity scattering is reduced to the minimum and the mean free path at these low temperatures will be limited by the linear dimensions of the sample only. Phonons, under such conditions, will propagate ballistically.

Experimental measurements on thermal conductivity for niobium which is a super conductor, have shown that the thermal conductivity at very low temperatures is proportional to T^3 It is further established that the thermal conductivity at low temperatures is highly anisotropic, being higher along symmetry axes than along other

directions. Measurements of silicon and calcium fluoride in the boundary-scattering regime have demonstrated anisotropes upto 50% for silicon and 40% for calcium fluoride. All these facts show that at these low temperatures, phonons propagate ballistically rather than diffusively.

As stated earlier, the elastic anisotropy of crystals results in the deviation of the group velocity vector from that of the wave vector. The energy flux is no longer collinear with the wave vector. In their heat pulse experiments, Taylor *et al*[21] reported very large differences in the intensity of phonons of different polarizations propagating ballistically in substances like Lithium fluoride or Pottasium chloride. When phonons were excited in a given region, the energy flow was enhanced in certain directions and decreased in other directions, even though the original angular distribution of the wave vectors was uniform. This channelling effect is called 'phonon focussing' in the literature[22,23]. Phonon focussing occurs when the direction of the group velocity varies more slowly than in an isotropic medium. The energy flow is generally higher along cuspidal edges or symmetry directions, though high phonon focussing occurs along non-symmetry directions too. The channelling effect of the phonons significantly affects the thermal conductivity, which is found to be anisotropic for cubic crystals at very low temperatures.

The phonon focussing effect is beautifully demonstrated by the heat pulse experiments conducted by various workers. In these experiments, a thin metallic film is coated on one surface of a crystal and phonons are generated by passing a short electrical or laser pulse over the film. The phonons arriving at the opposite face of the crystals are detected by a fast superconducting bolometer. Pulses due to phonons of different polarization arrive at the detector at different times and can be studied independently. von Gutfeld and Nethercot[24] detected the arriving phonons by a thin metal alloy film biased near its superconducting transition temperature. Variation in the resistance of the film is a sensitive probe of arriving heat pulse. In the imaging technique developed by Northrop and Wolfe[25], the heat pulse was generated by a pulsed laser beam and their bolometer at the opposite face consisted of a large array of identical detectors. The phonons propagate ballistically and the three pulses detected in the experiment correspond to the longitudinal, fast and slow shear modes.

Even though the hot region in all the heat pulse experiments is created as an incoherent source of phonons with isotropic angular distribution of wave vectors, the corresponding distribution of the group velocity vectors showed high anisotropy. Phonons are focussed in certain directions and defocussed in othr directions. Maris[26] pointed out that a phonon magnification factor A can be defined by taking the ratio of the solid angles in the wave vector space to the solid angle in the ray space q_s, (*i.e.*)

$$\frac{1}{A} = \frac{d\Omega_s}{d\Omega q} = \frac{\sin\theta_s\, d\theta_s\, d\phi_s}{\sin\theta\, d\theta\, d\phi}$$

The enhancement factor A is proportional to the phonon energy flux. Phonon energy emenating from a heated point source in the crystal is concentrated along directions for which A is large. The phonon magnification factor was computed for a large number of crystals by Maris, McCurdy and others by evaluating the above ratio numerically. Since the directions θ_s and ϕ_s of the group velocity vector are functions of the polar angles (θ, ϕ) of the wave vector, it was pointed out by Jacob Philip and the present author[27] that the ratio $d\theta_s\, d\phi_s / d\theta\, d\phi$ is none other than the Jacobian (J) of the transformation $\partial(\theta_s, \phi_s)/\partial(\theta, \phi)$ between the variables (θ_s, ϕ_s) and (θ, ϕ). Since mathematical expressions could be derived for the components of the group velocity vector in terms of the wave vector, it follows that the amplification can be evaluated analytically and is given by

$$\frac{1}{A} = J\frac{\sin\theta_s}{\sin\theta}$$

With the aid of a computer, the magnification $A(\theta, \phi)$ can be evaluated for different directions for any crystal. Numerical calculations show that the phonon magnification factor can be as

high as 10^3 for certain directions in crystals. The magnification has been found to be high for symmetry directions though it is not restricted to them, and large values have been noticed for other non-symmetry directions too. To compare the calculated values with experimental results, it is often convenient to study $A(\theta_s, \phi_s)$ rather than $A(\theta, \phi)$. This could be achieved by sorting the computer output for $A(\theta, \phi)$ in ascending values for the parameters θ_s or ϕ_s.

The method of ballistic phonon imaging devised by Northrop and Wolfe enables to produce a two dimensional map of the phonon intensities emanating from a point source and to correlate the observed intensities with geometric theory. They had been able to map the complicated topological features of the energy surface which exhibits ramps and ridges. By applying catastrope theory to the energy surface, Taborek and Goodstein[28] concluded that the singularities exhibited by the energy surface are of the fold and cusp varieties. They showed besides that these are in fact the two possible topological type of singularities for all crystals including crystals of lower symmetry.

In figure 9, we reproduce the ballistic phonon image for Germanium given by Northrop and Wolfe. Bright regions in the figure indicates high phonon flux impinging on the (001) face of the crystals. The point source of the phonons is situated at the centre of the opposite face of the crystal. Figure 10 is another three-dimensional representation of the image given in the previous figure. The ramp and ridge structures exhibited by the energy surface are clearly brought out by this figure.

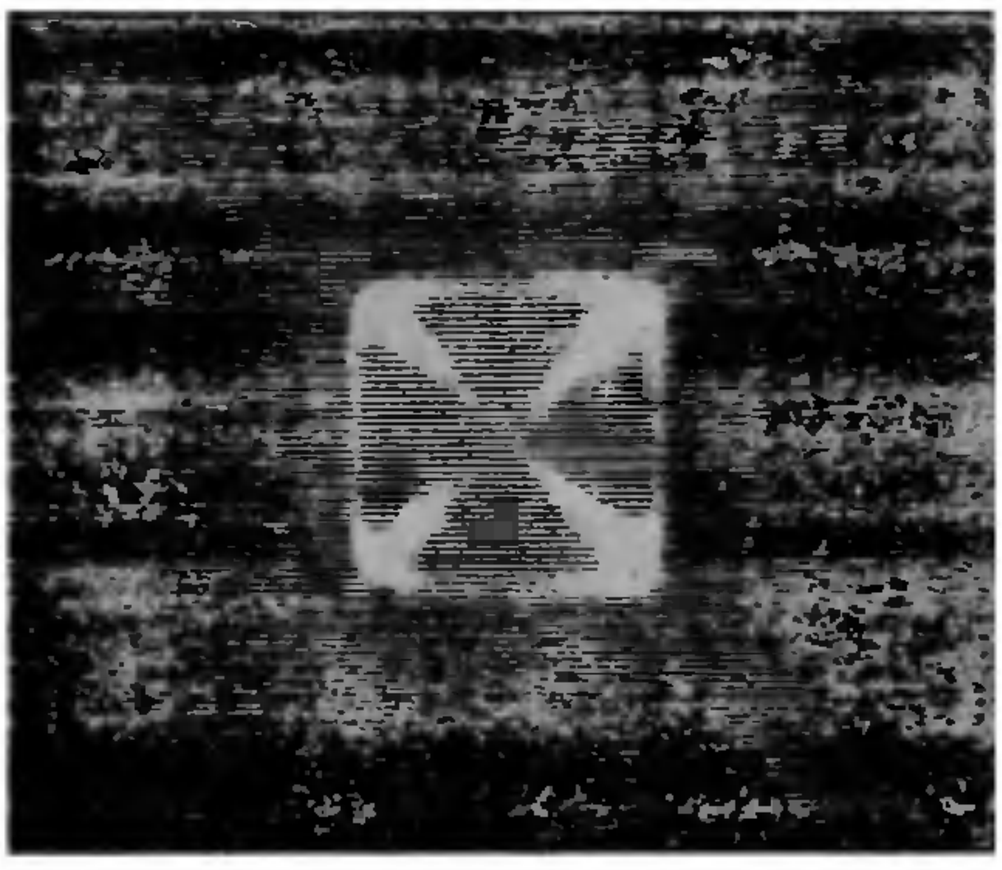

Figure 9. Ballistic phonon image for Germanium (after Northrop and Wolfe).

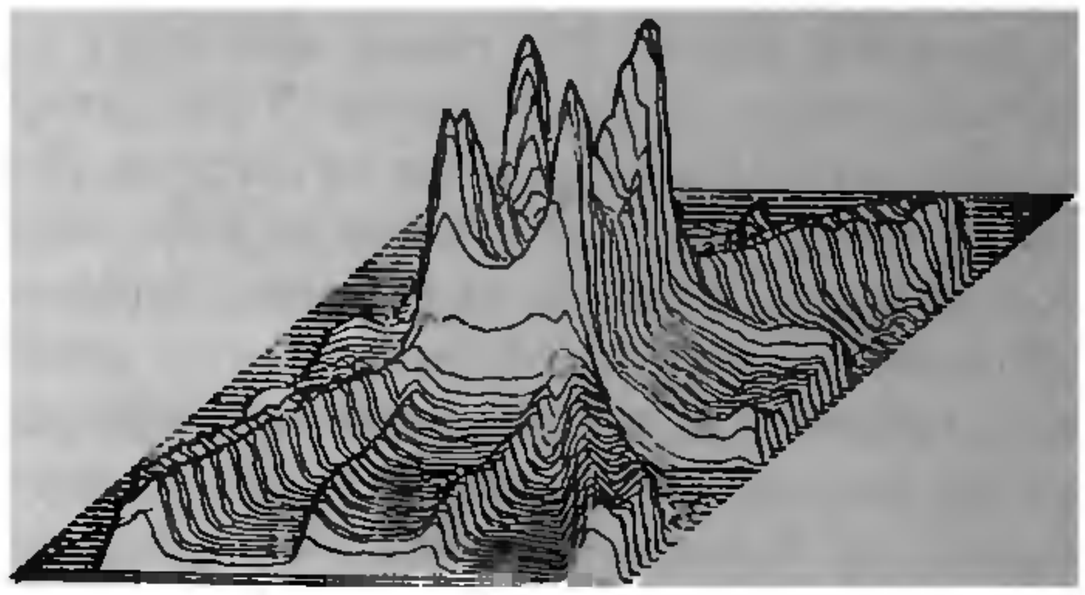

Figure 10. Three dimensional representation of the ramp and ridge structures exhibited by the energy surface. (After Northrop and Wolfe).

8. SECOND SOUND AND SOLITONS

A part from the heat pulse experiments, other areas hotly pursued in the subject relate to the second sound[29] and solitons[30] in solids. In second sound, heat propagates in a wavelike fashion unlike the ordinary diffusive heat conduction. Second sound was predicted by Landau[31] for superfluid helium on the basis of the two fluid theory of helium II. Since then there has been a constant look out for the existence of second sound in solids Acherman *et al.*[32] observed first the propagation of second sound in solid 4 He and observations of S. S. have been reported besides for sodium fluoride and bismuth. The propagation of the pulse in the heat pulse experiments is sensitive to the temperature. At very low temperature, the pulse propagates ballistically whereas for high T, the pulse travels in a diffusive manner. Narayanamurti and Varma[33] observed a secondary pulse of varying shape and velocity for intermediate temperature, which is interpreted as second sound. The propagation of solitons or finite amplitude waves in crystals is another area which is gaining momentum. A distinguishing feature of solitons is that two solitons can cross each other and reemerge without any distortion in shape or amplitude. One can confidently hope that

research in ballistic pulses, solitons and second sound will unfold new dimensions to this rich subject with multiple facet, which is still not closed but looks only brighter.

1. Auld, B. A., *Acoustic fields and waves in solids.*, (John Wiley New York), Vol. 1, 1973.
2. Staudt, J. H. and Cook B. D., *J. Acoust. Soc. Am.*, 1967, **41,** 1547.
3. Philip, J. and Viswanathan, K. S., *Pramana*, 1977, **8,** 348.
4. Narasimha, Iyer, V. and Viswanathan, K. S., *Pramana.*, 1981, **17,** 135.
5. Musgrave, M. J. P., *Acta Crystallogr.*, 1969, **7,** 265.
6. Viswanathan, K. S., *Indian J. Pure Appli. Phys.*, 1969, **7,** 265.
7. De Klerk J. and Musgrave M. J. P., *Proc. Phys. Soc.*, 1955, **68,** 81.
8. Papadakis, E. P. D., *J. Appl. Phys.*, 1963, **34,** 2163.
9. Pine, A. S., *Phys. Rev.*, 1970, **B2,** 2049.
10. Joffrin, J. and Levelut, A., *Solid State Commun.*, 1970, **8,** 1573.
11. Viswanathan, K. S., *Solid State Commun.*, 1979, **31,** 725.
12. Aigrain, P., *Proc. Int. Conf. Semi Conductor Physics Prague*, 1960, p. 224.
13. Kaner, E. A. and Skobov, V. G., *Plasma effects in metals—Helicons and Alfven waves* (Taylor and Francis Ltd, London) 1971.
14. Grimes, C. C. and Buchsvaum, S. J., *Phys. Rev. Lett.*, 2964, **2,** 357.
15. Viswanathan, K. S., *J. Phys. F. Metal Phys.*, 1975, **5,** 107.
16. Viswanathan, K. S., *J. Phys. F. Metal Phys.*, 1976, **6,** 993.
17. Sekar, R. and Viswanathan, K. S., *J. Phys. F. Metal Phys.*, 1978, **8,** 1099.
18. Idiculla R., and Viswanathan, K. S., *Can . J. Phys.* 1979, **57,**
19. Idiculla, R. and Viswanathan, K. S., *Pramana.*, 1980, **14,** 1.
20. Idiculla, R. and Viswanathan, K. S., *J. Phys. F. Metal Phys.*, 1981, **11,** 1635.
21. Taylor, B., Maris, H. J. and Elbum, C., *Phys. Rev.*, 1971, **B3,** 1462.
22. McCurdy, A. K., *Phys. Rev.* 1974, **9,** 466.
23. McCurdy, A. K., Maris, H. J. and Elbum, C., *Phys. Rev.*, 1970 **B2,** 4077.
24. Von Gutfeld, R. J. and Nethercot, A. H., *Phys. Rev. Lett.*, 1964, **12,** 641.
25. Northrop G. A. and Wolfe, J. P., *Phys. Rev.* 1980, **B22.**
26. Maris, H. J., *J. Acoust. Soc. Am.*, 1971, **50,** 812.
27. Jacob Philip, and Viswanathan, K. S., *Phys. Rev.* 1978, **B17,** 4969.
28. Taboreck, P. and Goodstein, D., *J. Phys.*, 1979, **C12,** 4737.
29. Beck, H., *Second sound and related phenomena in dynamical properties of solids.*, (Eds. G. K. Horton and A. A. Maradudin) North Holland, Vol. 2, 1975.
30. *Solitons and condensed matter Physics.*, (eds. A. R. Bishop and T. Schneider) Springer Verlag, Berlin, 1978.
31. Landau, L. D., *Zh. E. T. F.* 1941, **11,** 592.
32. Ackerman, C. C. *Phys. Rev. Lett.* 1966, **16,** 789.
33. Narayanamurti, and Varma, C. M., *Phys. Rev. Lett.*, 1970, **25,** 1105.